HEFAT2012
9th International Conference on Heat Transfer, Fluid Mechanics and Thermodynamics
16 – 18 July 2012
Malta

NUMERICAL ANALYSIS OF MIXING GUIDE VANE EFFECTS ON PERFORMANCE OF THE SUPERSONIC EJECTOR-DIFFUSER SYSTEM

Fanshi Kong, Yingzi Jin and Heuy Dong Kim*
*Author for correspondence
School of Mechanical Engineering,
Andong National University,
Andong, 760-749,
South Korea,
E-mail: kimhd@andong.ac.kr

ABSTRACT

Supersonic ejector-diffuser system makes use of primary stream with high speed and high pressure to propel the secondary stream through pure shear action. It has many advantages over other fluid machinery such as no moving parts and no direct mechanical energy input. That's why ejector-diffuser system has been used in many engineering industrial applications such as air propulsion and ejector refrigeration. The ejector-diffuser system also can be considered as the most important device of the solar seawater desalination.

Generally speaking, the flow field in the ejector-diffuser system is very difficult to be predicted due to the complicated turbulent mixing, compressibility effects and even flow unsteadiness. Many works have been done in the past years to achieve a higher efficiency and improve the performance of the ejector system, but not yet satisfactory, compared with that of other fluid machinery. Considering the complexity and difficulty on the researching, how to enhance the performance of ejector-diffuser system effectively became a significant task. In the present study, several mixing guide vanes were installed at the inlet of the secondary stream of the ejector-diffuser system for the purpose of the performance improvement. The present study aim is to lessen the negative effects on the secondary stream and get a higher level in both pressure recovery and entrainment ratio.

A CFD method based on Fluent has been applied to simulate the supersonic flows and shock waves inside the ejector. Numerical analysis results of the mixing guide vane effects were validated with experimental data in the previous work. The comparison of ejector performance with and without the mixing guide vane was obtained and optimal position of mixing guide vane is discussed to increase the performance. The operation characteristics of the ejector system with different numbers of inlet guide vanes are analyzed in detail. The ejector-diffuser system performance is discussed in terms of the entrainment ratio, ejector efficiency, pressure recovery as well as total pressure loss.

INTRODUCTION

Supersonic ejector-diffuser system can be used in many complex progresses. It can be considered as the most important component in such industrial applications as solar desalination [1], refrigeration [2,3], rocket propulsion and vacuum pump [4]. This system makes use of high pressure stream to force another stream into the mixing chamber through pure shear action. If the primary stream velocity is high enough, the ejector can be called as supersonic ejector, where the Mach number of primary stream inlet is more than 1. Therefore, strong driving force is created to propel the secondary stream into the mixing section. Two streams mix up in the mixing chamber and exchange kinetic energy and potential energy completely. The mixing stream pressure is elevated again in the following diffuser section and exhausts with a higher pressure than the previous stream.

There are two important coefficients to describe the performance except system efficiency: mass flow ratio of two streams and the pressure recovery between inlet and outlet [5]. Many researching works have been done in the past years to increase the performance of the ejector, but results were still unsatisfactory, compared with other industrial machineries [6,7]. Considering the complexity and difficulty on the researching, how to enhance the performance of ejector-diffuser system effectively became a significant task.

Keenan JH et al. [8,9]came up with a new designing theory based on one-dimensional ejector. It was widely used in the calculation of axial coefficients of ejector-diffuser system, such as momentum, kinetic energy and pressure exchanging. But the calculating operation was very strict and limited, not suitable for indeterminable ejector structure. Recently, one research by Eames IW et al. [10] put forward a new proposal combined advantages of previous ejectors. The results had a good

increment of critical back pressure and efficiency. Munday J.T. [11] had a good design scheme of an active area of the mixing section, which could be redefined as another important parameter to describe the ejector operating status. In the past decades, Many researchers have done many significant works and got a lot of good results based on geometrical optimization, but the optimization of internal structure has got little attention [10,11]. In the Texas A&M University, a researching team pointed out a good optimal method using a mixing guide vane installed at the inlet of ejector [14]. A productive experimental work of this ejector has been made by Manohar [15], and Somsak W. [16] has finished the basic CFD analysis in his doctoral dissertation. From their experimental results, the mixing guide vane effects were good at pressure recovery increment of ejector-diffuser system. But the mass flow rate of secondary stream was decreased due to the negative influence on the ejector inlet. Similar experimental appliance model was illustrated schematically in the Figure 1.

In this paper, a CFD work was applied with a supersonic ejector-diffuser system which was used in the Somsak's work [16]; the geometrical model was applied in the solar desalination industrial. The schematic of supersonic ejector-diffuser system in a solar desalination circulation was illustrated in the Figure 2. The ejector-diffuser system can be used in reducing the pressure of evaporator and propelling incondensable gas into the condenser [1,17]. Generally speaking, the working fluid used in the solar desalination process was vapour only, but ideal gas was used in the present CFD works. Because they can get a similar result after simulation progress, while the model based on ideal gas was easier to be built and less computational time is needed.

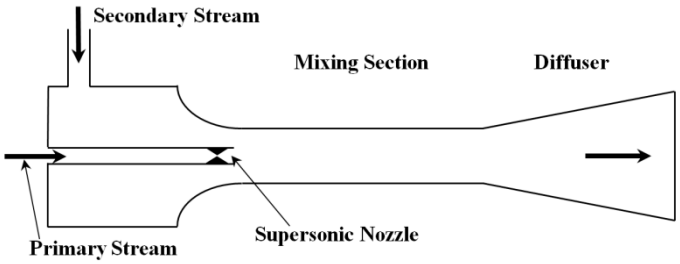

(a) Without mixing guide vane

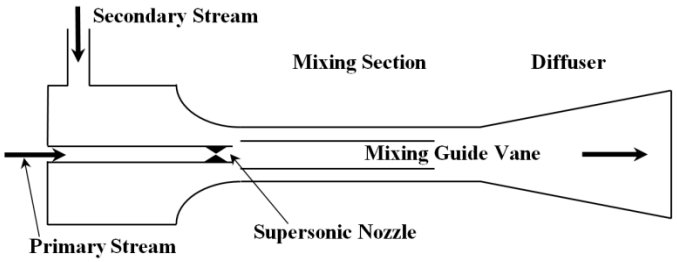

(b) With mixing guide vane

Figure 1 Geometrical schematic of supersonic ejector-diffuser system

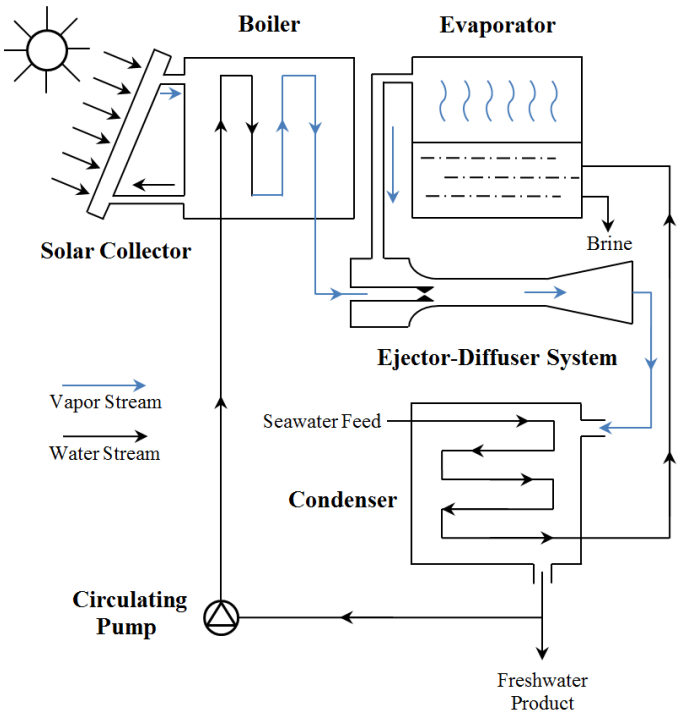

Figure 2 The supersonic ejector-diffuser system in a solar desalination circulation

NOMENCLATURE

A	[m^2]	Cross-sectional area of supersonic nozzle exit
D	[mm]	Diameter of particular position
L	[mm]	Length of the mixing guide vane
L_s	[mm]	Distance between nozzle exit and mixing guide vane
M	[-]	Mach number at primary stream nozzle exit
P	[Pa]	Pressure
R	[J/kg•K]	Gas constant
Rm	[-]	Entrainment ratio: Ratio of two mass flow rates of primary and secondary stream
$Rm`$	[-]	Entrainment ratio with mixing guide vane
T	[K]	Temperature
V	[m/s]	Velocity of primary stream
x	[m]	Cartesian axis direction
y	[m]	Cartesian axis direction

Special characters

η	[-]	Total pressure loss ratio: Percentage difference between total pressure at the primary stream nozzle exit and exit of ejector-diffuser system
$\eta`$	[-]	Total pressure loss ratio with mixing guide vane
γ	[-]	Ratio of specific heats
$\dot{m}$	[kg/s]	mass flow rate
ΔP	[Pa]	Pressure recovery: Difference between static pressure at the secondary stream inlet and exit of ejector-diffuser system
$\Delta P`$	[Pa]	Pressure recovery with mixing guide vane

Subscripts

1	1st: Values at supersonic nozzle exit
2	2nd: Values at Secondary stream inlet
e	Exit: Supersonic ejector-diffuser system exit
M	Mixing chamber of ejector-diffuser system
s	Static values
t	Total values
V1	Front end of the mixing guide vane
V2	After end of the mixing guide vane

In the present work, a CFD method based on Fluent has been applied to simulate the ejector internal flow. The geometrical model was created exactly same with the experimental apparatus. A mixing guide vane was installed in the ejector to elevate the performance of ejector. Optimal analyses were put into use to lessen the negative influence on the secondary stream. The objective of this research is to get an advanced value in both entrainment ratio and pressure recovery under the mixing guide vane influence. The supersonic ejector-diffuser system geometry is schematically shown in Figure 1(a). And Figure 1(b) represents the original position of mixing guide vane. Optimal position of mixing guide vane was investigated based on different guide vane lengths and distances to supersonic nozzle exit. The ejector-diffuser system performance with and without mixing guide vane was compared.

COMPUTATIONAL MODEL

A typical ejector-diffuser system consists mainly 3 parts include a supersonic nozzle, a mixing chamber and a diffuser, which has been showed in the Figure 3. The ejector was built as a constant area ejector, with a constant mixing chamber area (CMA). This kind of ejector had a better compression ratio than another ejector with constant pressure mixing (CPM). In the present researching, a two-dimensional model was used with a symmetric axis. Similar results can be obtained from 3D model or full model, but need finer mesh cells and more computational time.

For the nomenclature of ejector, P_s was defined as static pressure while P_t represented the total pressure. Boundary conditions and operating pressures of inlet and exit were illustrated in the Figure 3. Indeed, the geometrical model of the ejector structure was stationary, while the parameters of mixing guide vane were changed to obtain the optimal position. The diameters of supersonic nozzle (D_1) and mixing section (D_M) were kept constant as 6.08mm and 84.56 mm. The total length of ejector-diffuser mixing chamber was approach to 14D.

Figure 4 represents the geometrical model of mixing guide vane. As the innovation of the optimal works, the mixing guide vane effects on performance of the ejector were discussed in terms of compression ratio, pressure recovery and total pressure loss. From the Figure 4, D_{V1} and D_{V2} were defined as the diameter of front end and after end of the mixing guide vane. The guide vane was built as a circular truncated cone, while D_{V1} and D_{V2} were not equal ($D_{V1} > D_{V2}$).

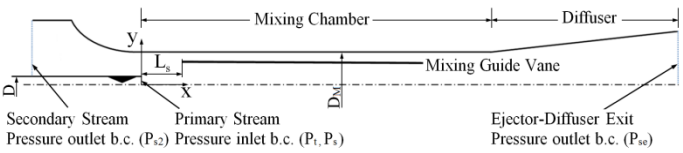

Figure 3 Schematics of the supersonic ejector and boundary condition settings

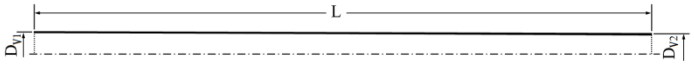

Figure 4 Geometry model of the mixing guide vane

Table 5 Adjustable parameters in different models

Model (a)	Model (b)	Model (c)	Model (d)	Model (e)
No guide vane	L_s=0D	L_s=1D	L_s=2D	L_s=3D
	Model (f)	Model (g)	Model (k)	
	L=14/4 D	L=14/2 D	L=14 D	

Two adjustable values of mixing guide vane were varied to optimize the ejector-diffuser system. One is the length of mixing guide vane (L), Another is L_s which represents the distance between mixing guide vane and supersonic nozzle exit. Both values were illustrated in the Figure 3 and 4. Table 1 listed adjustable parameters in different models, all 8 models were numerical simulated in CFD works. In the first step, the optimal model under L_s effects was obtained, and then established new domain under L effects using the optimal L_s value. Optimal operating values were given after comparison of simulating results of these models.

NUMERICAL METHOD

Commercial software Gambit was used in the present research to create mesh domain. A structure mesh was employed in this case and quadrilateral cells were used in the mesh creation. Boundary layer effects were considered by making finer grid densely clustered close to the walls. Different mesh qualities were compared in terms of percentage deviation and computational time. Grid-independent solutions were showed in the table 1 compared of 3 different mesh numbers. All these cases were simulated based on the model a, without mixing guide vane installed. The percentage deviation was the difference of total mass flow rates between the CFD analysis and experimental results. From Table 1 of Grid-independence check list, the difference between CFD analysis and experimental results was less than 5%. Hence, the grid independence was also checked. The computational domain with 232,325 cells was chosen because of its less computational time and more accurate result.

Table 6 Grid-independence check

Grid numbers	$\dot{m}_e$ (CFD)	$\dot{m}_e$ (Exp.)	Percentage deviation
156,527	0.639 kg/s	0.67 kg/s	4.62 %
232,325	0.684 kg/s		2.18 %
345,235	0.685 kg/s		2.30 %

Table 7 Computational boundary conditions

	Case (1)	Case (2)	Case (3)	Case (4)	Case (5)
V (m/s)	411	449	490	528	563
M	1.20	1.30	1.43	1.54	1.66
P_t (MPa)	0.25	0.29	0.35	0.41	0.48

For the CFD software, ANSYS Fluent 13.0 was chosen to simulate internal flows of ejector. Ideal gas was chosen as the working fluid in all cases. A finite volume scheme and density-based solver with coupled scheme was applied in the computational process. Standard k-ω turbulent model was used considering the accuracy and stability of this turbulent model. Second-order upwind scheme was used for turbulent kinetic energy as well as spatial discretizations.

Total pressure boundary conditions were used at the supersonic primary stream nozzle exit. The inlet and outlet of ejector were extended to stabilize the computational results. Pressure outlet boundary conditions were used at both inlet and outlet of the ejector. Therefore, the secondary stream inlet and ejector exit were taken from ambient conditions of an atmospheric pressure.

Initial values can be calculated in these equations:

$$\frac{P_s}{P_t} = \left(1 + \frac{\gamma-1}{2}M^2\right)^{\frac{-\gamma}{\gamma-1}} \quad (1)$$

$$\frac{T_s}{T_t} = \left(1 + \frac{\gamma-1}{2}M^2\right)^{\frac{-\gamma}{\gamma-1}} \quad (2)$$

$$M = \frac{V}{\sqrt{\gamma RT}} \quad (3)$$

$$\dot{m} = \rho VA \quad (4)$$

RESULTS AND DISCUSSION

Due to the characteristics of compression flow, shock wave should occur in the internal flow section when the Mach number is larger than 1. In this paper, the ejector has a special feature that the length-diameter ratio is very high, the total length of mixing section is almost 15D, and the total length of ejector is nearly 28D. That is a typical ejector structure which has a shorter mixing process compared with the long geometrical model. Primary stream and secondary stream were mixed up fully in the early beginning in the mixing chamber. Furthermore, a very small diameter of supersonic nozzle can be found in the geometrical model. Considering all these features and characteristics of the supersonic ejector-diffuser system, the researching upon the shock system are more significant and meaningful, especially the shocks around the nozzle exit of primary stream. Besides, after compared all different contours graphics, the contours of Mach number showed more obvious results of shock system. The contours of Mach number with all 8 models were found in the Figure 5. All these figures were based on case 5 with a Mach number of 1.66, which showed the better results in pressure recovery increment and entrainment ratio variation.

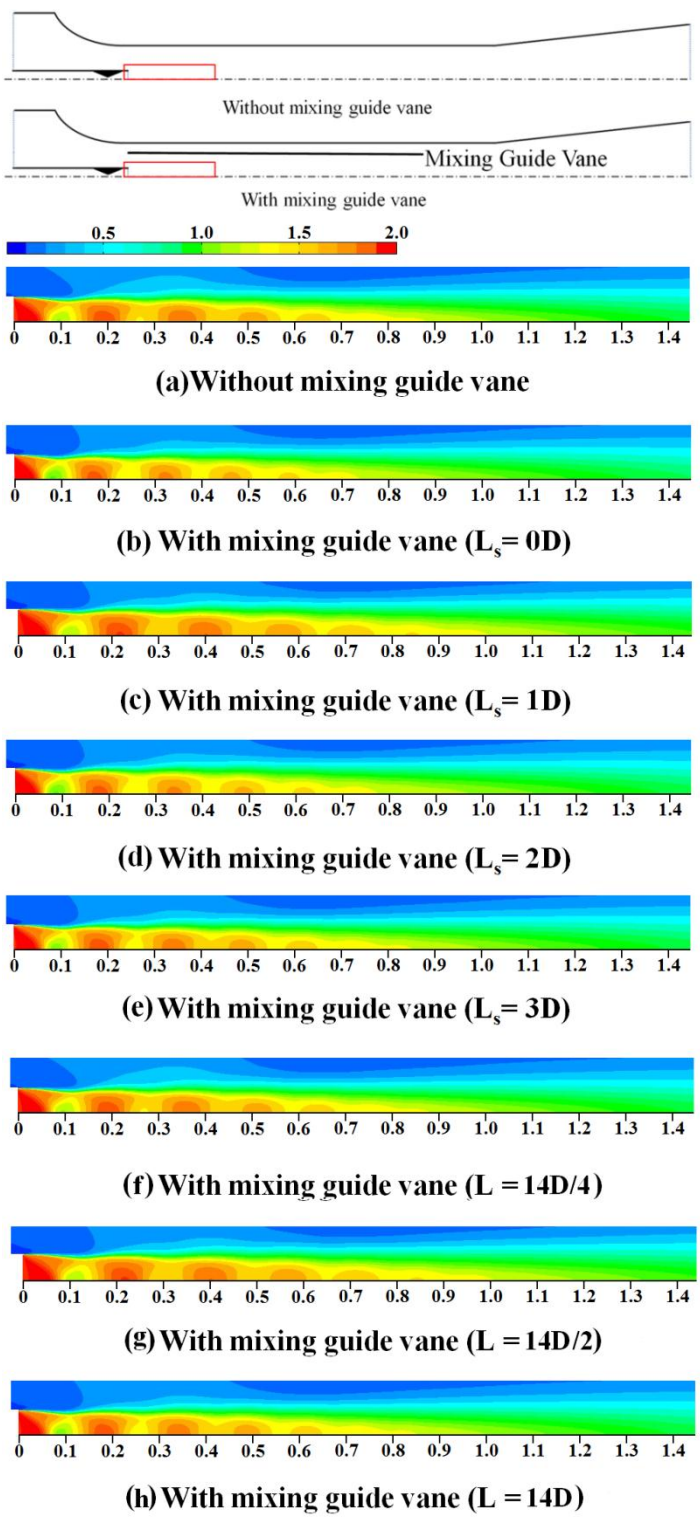

Figure 8 Contours of Mach number for case 5

Fig. 5 shows the contours of Mach number around the primary stream nozzle exit for case 5. The upper figures show the position of the Mach number variation, marked in a red quadrilateral. For other figures, the first field represents the computational results for the model (a) without mixing guide vane. At the same time, the results for the models with a mixing guide vane were shown in the other fields (b-h). The scales of these contours were exactly same to each other, in order to compare these 8 models in a same standard. All these figures were illustrated in a same continuous variation of the distance begin from the supersonic nozzle exit, from 0D to 1.4D.

From these contours of Mach number, a strong first shock can be found in all the cases, and continuous shock cells were created in the next step. The differences were concentrated on the mixing guide vane effects of shock waves. From the graphics of model (b-e), the mixing guide vane effects were discussed in differences of L_s value. The model (c) with a distance of 1D showed better influence on the shock system, and more shock cells can be found in this model; another model with a mixing guide vane distance of 0D (model b) showed negative influence on the shocks creation, more weaker shock waves can be obtained. The model (b) had a too longer mixing guide cane to involve more secondary stream and then lead to negative effects on the shock system. Hence, it should be easy to get an opinion that a longer sub-critical area created a better promotion in the entrainment ratio [18]. For other cases like model d and model e, the numerical results were given similar with the model without mixing guide vane.

As the results of other results under the lengths effects, all 3 models were illustrated based on the L_s=1D. Actually, the L effects upon shock systems were not obvious as the L_s value. In author's opinion, the shock system were influenced by front end of the mixing guide vane, the length had no important effects like them. But from these 3 graphics, the model f with the L=14D/2 showed the better results of the influence on the shock system.

DIMENSIONLESS ANALYSIS

In this part, the performance of the ejector-diffuser and effects of the mixing guide vane were discussed in terms of entrainment ratio, pressure recovery and total pressure loss ratio. All these coefficients were indispensable values to describe the system performance.

Entrainment ratio (Rm) is one of the most important parameters mentioned above, which can be represented by the following equation:

$$\mathrm{Rm} = \frac{\text{mass flow rate of secondary flow}}{\text{mass flow rate of primary flow}} \qquad (5)$$

In the present study, the entrainment ratio under L_s effects is shown in Figure 6 while the parameter under L effects is illustrated in Figure 7. The effects of mixing guide vane and the influence on the system can be easily found from both figures. All computational results based on 5 cases and 8 models were included, the cases of different Mach numbers were compared. The effects of mixing guide vane geometry were investigated.

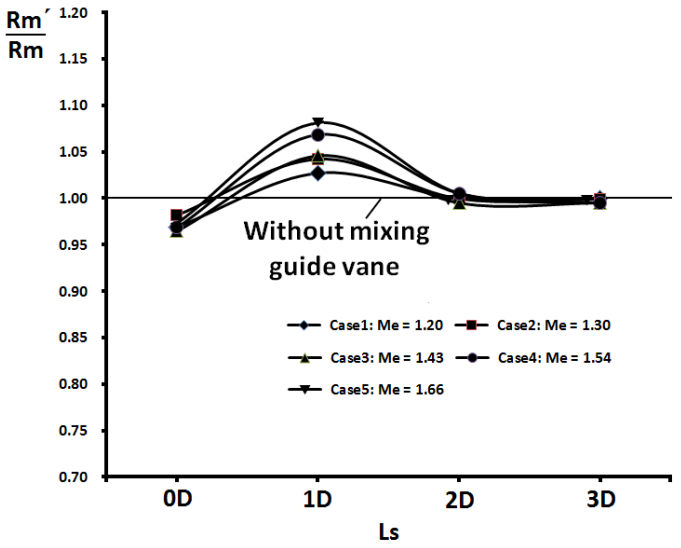

Figure 9 Entrainment ratio under L_s effects

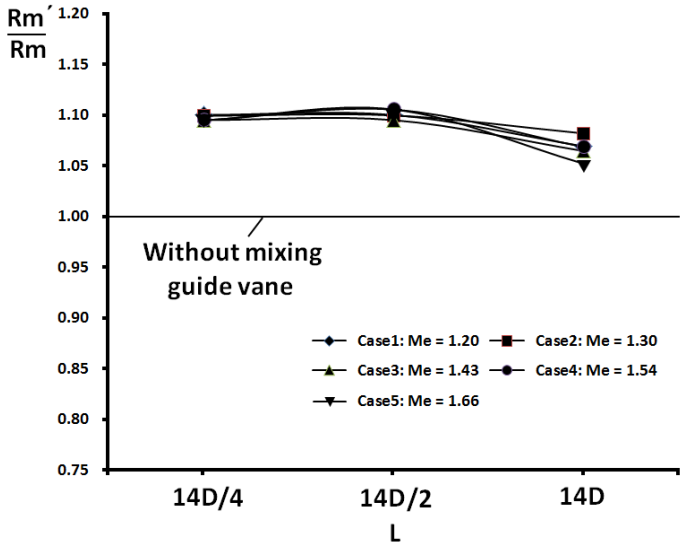

Figure 10 Entrainment ratio under L effects

In the Figure 6, the entrainment ratio under L_s effects was shown. Along the L_s increase, different effects of mixing guide vane were shown: the mixing guide vane with L_s=0D had a negative influence on the ejector, the decrement is 3.9%; the model with L_s=1D had a positive effect, with an increment of Rm as 5.3% in average and 8.1% in maximum; other models with L_s=2D and L_s=3D had gat resemble results compared with the model without mixing guide vane. These results demonstrated the analysis of the contours of Mach number. At the same time, when M ranges from 1.20 to 1.66, it was found that the difference of entrainment ratio tended to increase. From the comparison of these models under different mixing guide vanes, the area of secondary inlet section and the productive capacity of primary stream were changed.

Figure 7 represents the entrainment ratio under L effects. All the models showed better results because all these models geometry were created with L_s=1D. Following the position moving, the models with L=14D/4 and L=14D/2 showed

similar results with model (c), and the model with L=14D/2 showed better results compared with another model. The increment of Rm with the optimal model was 6.8%, and the maximum value of increase achieved was 8.8%. Generally speaking, under the guide vane influence, more flow vortexes were generated and introduced into the stream. Therefore, shock system was changed and introduced more secondary stream into the ejector-diffuser system, which effectively enhanced the performance of the ejector-diffuser system.

Pressure recovery (ΔP) can be defined as the difference between static pressure at the secondary stream inlet (P_{s2}) and static pressure at the outlet of ejector-diffuser system (P_{se}). Total pressure loss ratio (η) can be considered as the difference between total pressure at the nozzle exit (P_t) and total pressure at the outlet of ejector-diffuser system (P_{te}). The calculations of pressure recovery (ΔP) and total pressure loss ratio (η) can be represented by the following equation:

$$\Delta P = P_{se} - P_{s2} \quad (6)$$

$$\eta = \frac{P_t - P_{te}}{P_t} \times 100\ (\%) \quad (7)$$

The pressure recovery under L_s effects is shown in Figure 8. The pressure recovery under L effects is illustrated in Figure 9. The effects of mixing guide vane geometry were also investigated in these graphics, based on 5 different operating conditions and 8 different adjustable values.

In the Figure 8, the pressure recovery under L_s effects was illustrated. Along the Mach number increasing, the pressure recovery became larger gradually. With the L_s increase, effects of mixing guide vane were shown in different ways, but all 4 models showed better results in pressure recovery than the model without mixing guide vane. Among them, the model with L_s=1D had a positive influence on the ejector, with an average increment of 18.6%, and the maximum amplitude was 25.0%. Figure 9 represented the pressure recovery under L effects. All the models showed resemble results compared with the model of L_s=1D. Considering all 3 cases, the model with L=14D/2 showed better results compared with another model. The increment of ΔP was 18.8% in average, and the maximum value of increase achieved was 25.3%. With a mixing guide vane, the energy transfer of mixing between two streams was increased effectively, which enhanced the pressure recovery of the ejector-diffuser system to higher level.

Fig. 10 showed the comparison of total pressure loss between with and without mixing guide vane. Along the L_s increasing, the negative influence on frictional force became weaker. That's why the total pressure loss was decreased along the L_s increasing, but still larger than the model without mixing guide vane. Although the mixing guide vane really helped to mix the primary & secondary stream, but the frictional force will be increased. Therefore, the mixing guide vane enhanced the total pressure loss of the ejector-diffuser system.

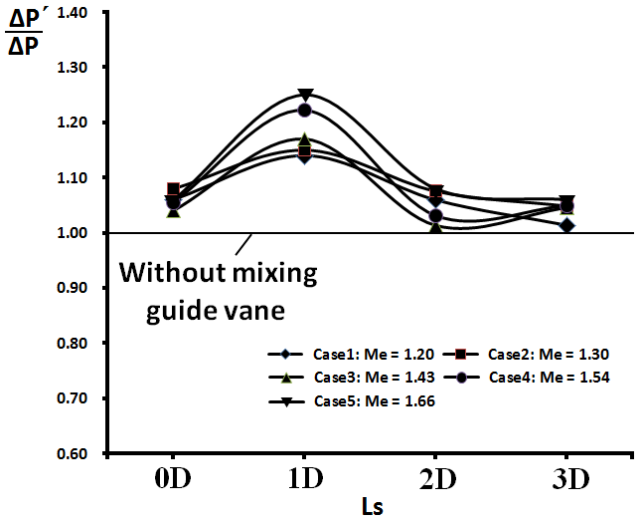

Figure 11 Pressure recovery under Ls effects

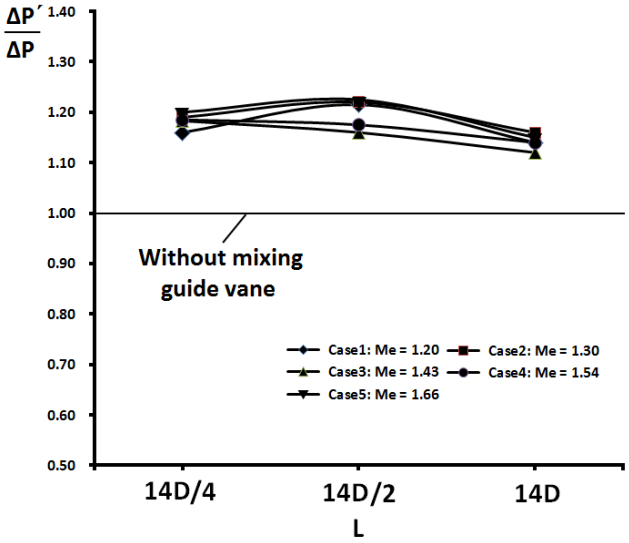

Figure 12 Pressure recovery under L effects

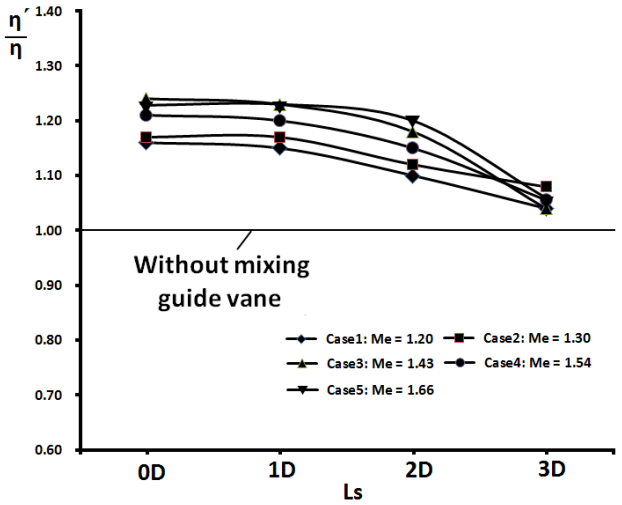

Figure 10 Total pressure loss with and without mixing guide vane

CONCLUSION

In the present paper, a computational method was carried to simulate the internal flow of an ejector-diffuser system. The mixing guide vane effects on the performance of the ejector were investigated. The optimal position and length of mixing guide vane were given. Both models with and without guide vane were compared. Numerical results were confirmed by previous experimental data.

4 different positions and 3 lengths of mixing guide vane were involved in the present research. As the conclusion of an optimal model, the mixing guide vane with L_s=1D and L=14D/2 showed better results: the entrainment ratio was improved 6.8% in average, and the maximum 8.8%. This model also leaded to a better pressure recovery of 18.8% in average and got the largest increase in amplitude of 25.3%.

At the same time, all 7 models with mixing guide vane showed better results to increase the pressure recovery. On the other hand, total pressure loss ratio was increased under the mixing guide vane influence. Further work is going on to optimize the mixing guide vane thickness and numbers.

REFERENCES

[1] Sandeep P., Farid M.M., Selman J.R., and Said H., Solar deslination with a humidification-dehumidification technique-a comprehensive technical review, *Desalillation*, Vol.160, 2004, pp.167-186

[2] Chunnanond K. and Aphornratana S., Ejectors: applications in refrigeration technology, *Renewable & Sustainable Energy Reviews*, Vol.8, 2004, pp.129-155

[3] Huang B.J., and Petrenko V.A., Chang J.M., Lin C.P., Hu S.S., A combined cycle refrigeration system using ejector-cooling as the bottom cycle, *International Journal of Refrigeration*, Vol.24, No.3, 2001, pp.391-399.

[4] Senthil K.R., Mani A., and Kumaraswamy S., Analysis of a jet-pump-assisted vacuum desalination system using power plant waste heat. *Desalination*, 2005

[5] Rusly E., Aye L., Charters W.W.S., and Ooi A., CFD analysis of ejector in a combined ejector cooling system, *International Journal of Refrigeration*, Vol.28, 2005, pp:1092-1101

[6] Riffat S. B., and Omer S. A., CFD modelling and experimental investigation of an ejector refrigeration system using methanol as the working fluid, *Int. Jour. Energy Res.*, Vol.2, 2001, pp.25

[7] Reinke B., Neal M. and Gupta S. M., Flow inside a jet-ejector pump for vacuum applications, *Jour. Ind. Inst. Chem. Engrs.*, Vol.3, 2002, pp.44

[8] Keenan J.H., and Neumann E.P., A simple air ejector, *J Appl Mech-T ASME*, Vol.64, 1942, pp.75-81

[9] Keenan J.H., Neumann E.P., and Lustwerk F., An investigation of ejector design by analysis and experiment, *J Appl Mech-T ASME*, Vol.72, 1950, pp.299-309.

[10] Eames I.W., A new prescription for design of supersonic jet pumps: constant rate of momentum change method, *Appl Therm Eng*, Vol.22, 2002, pp.121-131

[11] Munday J.T., and Bagster D.F., A new theory applied to steam jet refrigeration, *Ind. Eng. Chem. Proc. DD*, Vol.4, 1997, pp.442-449

[12] Beithou N., and Aybar H.S.., High-pressure steam-driven jet pump-part I: mathematical modeling, *Journal of Engineering for Gas Turbines and Power*, Vol.123, 2001, pp.693-700

[13] Beithou N., and Aybar H.S., High-pressure steam-driven jet pump-part II: parametric analysis, *Journal of Engineering for Gas Turbines and Power*, Vol.123, 2001, pp.701-706

[14] Holtzapple M.T., High-efficiency jet ejector, Invention Disclosure, Texas A&M University, 2001

[15] Manohar D.V., Desalination of seawater using a high-efficiency jet ejector, Master Thesis, Texas A&M University, 2005

[16] Somsak W., CFD optimization study of high-efficiency jet ejector, Doctoral Dissertation, Texas A&M University, 2008

[17] Blanco J., Malato S., Ferna ́ndez-Iban˜ez P., Alarco ́n D., Gernjak W., and Maldonado M.I., Review of feasible solar energy applications to water processes, *Renewable and Sustainable Energy Reviews*, Vol.13, 2009, pp.1437-1445

[18] Amel H., Fran ̧ois H., S ́ebastien L., Jean-Marie S., and Yann B., CFD analysis of a supersonic air ejector. part II: relation between global operation and local flow features, *Applied Thermal Engineering*, Vol.29, 2009, pp.2990-2998